JACS
JOURNAL OF THE AMERICAN CHEMICAL SOCIETY
Article
pubs.acs.org/JACS

Light Controlled Reversible Inversion of Nanophosphor-Stabilized Pickering Emulsions for Biphasic Enantioselective Biocatalysis

Zhaowei Chen,[†,‡] Li Zhou,[†,‡] Wei Bing,[†,‡] Zhijun Zhang,[†,‡] Zhenhua Li,[†,‡] Jinsong Ren,*[,†] and Xiaogang Qu*[,†]

[†]State Key Laboratory of Rare Earth Resources Utilization and Laboratory of Chemical Biology, Changchun Institute of Applied Chemistry, Chinese Academy of Sciences, Changchun 130022, China

[‡]Graduate School of the Chinese Academy of Sciences, Beijing 100039, China

Supporting Information

ABSTRACT: In this work, by utilizing photochromic spiropyrans conjugated upconversion nanophosphors, we have successfully prepared NIR/visible light tuned interfacially active nanoparticles for the formulation of Pickering emulsions with reversible inversion properties. By loading a model enantioselective biocatalytic active bacteria *Alcaligenes faecalis* ATCC 8750 in the aqueous phase, we demonstrated for the first time that the multifunctional Pickering emulsion not only highly enhanced its catalytic performance but also relieved the substrate inhibition effect. In addition, product recovery, and biocatalysts and colloid emulsifiers recycling could be easily realized based on the inversion ability of the Pickering emulsion. Most importantly, the utilization of NIR/visible light to perform the reversible inversion without any chemical auxiliaries or temperature variation showed little damage toward the biocatalysts, which was highlighted by the high catalytic efficiency and high enantioselectivity even after 10 cycles. The NIR/visible light controlled Pickering emulsion showed promising potential as a powerful technique for biocatalysis in biphasic systems.

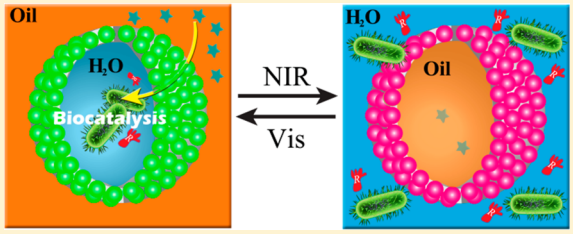

INTRODUCTION

Biocatalysts, such as enzymes and cells (e.g., microbe), have aroused a great deal of excitement in sustainable industrial chemistry owning to their overall high chemo-, regio-, and stereoselectivity under mild reaction conditions.[1−6] Despite such striking characteristics, biocatalysts have not been widely used because, in many cases, substrates of interest are only soluble in organic solvents, whereas biocatalysts typically prefer aqueous environment. So biocatalytic reactions are often performed in biphasic systems to enhance productivity. However, prolonged exposure of the biocatalysts to organic/aqueous interfaces would lead to reduced activity. Moreover, the reaction rate would be limited by the mass transport through the finite organic/aqueous interfacial areas. During the past decades, biocatalyst immobilization has been considered as the major breakthrough among the attempts to circumvent these problems.[1] A simple way to do this is the formation of surfactant stabilized water-in-oil (w/o) emulsions to protect biocatalyst against denaturation at the interface and increase the area between organic and aqueous phase.[7,8] Although promising, the deleterious effects of surfactants on biocatalysts and the problems involved in emulsion break for product separation and biocatalysts recycling impede the widespread application of the reverse micelle technology.[9]

Alternatively, Pickering emulsions, which are emulsions stabilized by colloidal nanoparticles, have proven to be versatile immobilization techniques that provide efficient encapsulation in structures whose size, permeability, mechanical strength, and compatibility can be easily controlled.[10,11] Generally, the wettability of the particle surface, described by the contact angle θ between the solid and the oil−water interface, establishes the type of emulsion formed.[12] Normally, hydrophobic particles ($\theta > 90°$) will reside in oil rather than in water so they will stabilize w/o emulsions; for hydrophilic particles ($\theta < 90°$), oil-in-water (o/w) emulsions will be more probable. In addition, the nanoparticles employed in the system can also confer the emulsions excess smart functional characteristics.[13−28] For instance, stimulus-responsive Pickering emulsions stabilized by switchable surface-active colloid particles have shown the ability to allow on-demand demulsification or phase inversion.[21−24] On the basis of these unique properties, Pickering emulsions strongly enhance the opportunities for biocatalytic reactions in biphasic reaction media,[11,17−21] which could be anticipated to easily control product separation, and biocatalyst and emulsifiers recycling. For example, Wu and other groups have applied Pickering emulsions with the encapsulation of catalytically active enzymes inside the water phase for biphasic reactions.[11,18−21] However, the immobilization of whole bacteria in reversible intelligent Pickering emulsions for biphasic biocatalysis remains elusive.

Recently, much effort has been paid to develop intelligent Pickering emulsions stabilized by surface-active particles that respond to specific triggers such as changes in pH,[22−24]

Received: March 28, 2014
Published: May 2, 2014

   dx.doi.org/10.1021/ja503123m | J. Am. Chem. Soc. 2014, 136, 7498−7504

Scheme 1. Schematic Illustration of the NIR/Visible Light Controlled Pickering Emulsions with Reversible Inversion Ability for Biphasic Enantioselective Biocatalysis

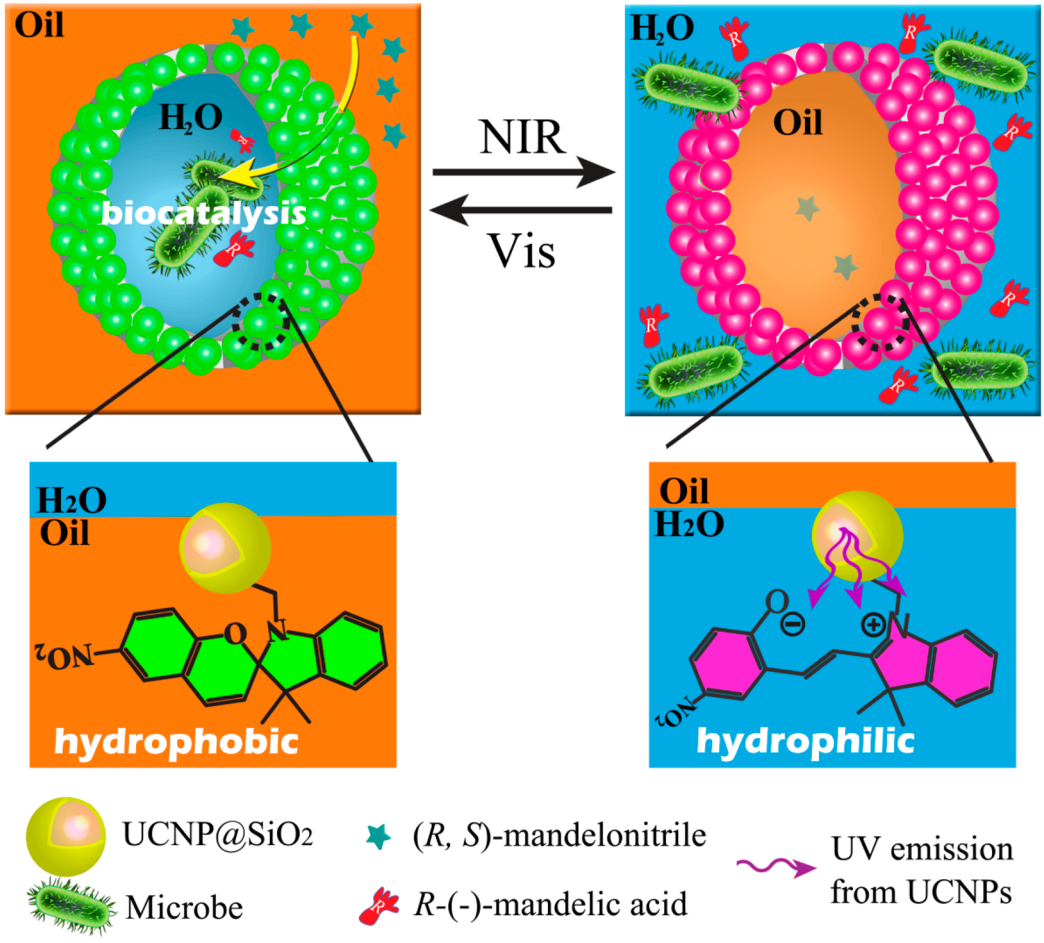

temperature,[15,16,21] salt concentration,[24] or carbon dioxide.[25] However, these processes are mainly based on in situ physicochemical stimuli, which would limit repeated switching cycles for biocatalytic applications. Furthermore, biocatalysts typically require specific reaction conditions, for example, pH value, ionic strength, and temperature. Therefore, more convenient approaches that can tune particle surfaces though a remote control are urgently needed. Light is an excellent trigger because of its easy mediation of wavelength, intensity, illuminated area, and duration. Especially, for biological process, multiphoton excitation with NIR light has been presented as a practical solution to the issues associated with UV light, given that NIR light is less damaging toward biospecimens.[29−34] However, to the best of our knowledge, reports on NIR light controlled surface switch of particles in Pickering emulsions for biocatalysis have not been found in literature so far.

Lanthanide-doped upconversion nanoparticles (UCNPs) have received much attention in recent years in material science. These nanoparticles can emit UV, visible, and/or near-infrared (NIR) light upon NIR excitation (typically 980 nm) with a large anti-Stokes shift. UCNPs have several outstanding features such as narrow emission bandwidth, long luminescence lifetimes, higher chemical and photo stability, lower background light, and excellent biocompatibility. These unique properties make UCNPs as a kind of nanophosphors that are attractive for applications in fields such as flat-panel displays, photonics, photovoltaics, and biological labeling and imaging.[35−44] Although the development of functional UCNPs shows great promise in photonic technology, the further expansion of their application in the field of biocatalysis related sustainable chemistry still remains a big challenge.

Herein, we propose a conceptually new approach: by utilizing photochromic spiropyran conjugated upconversion nanophosphors as colloidal emulsifiers, a novel NIR/visible light controlled Pickering emulsion with reversible inversion ability could be easily established and applied for biocatalytic applications. As shown in Scheme 1, upon absorption of NIR excitation, the UCNPs emit photons in the UV region that, in turn, induce the formation of ring-open spiropyran form. This isomerization process can be reversed by exposure to visible light. Such transformations make the hydrophilicity/hydrophobicity of UCNPs' surface switchable, thus driving the emulsion inversion. By loading a model bacteria *Alcaligenes faecalis* ATCC 8750 in the aqueous phase, we demonstrated for the first time that this Pickering emulsion not only enhanced its catalytic performance, but also relieved the substrate inhibition effect. Moreover, owning to the inversion ability of the emulsion, product recovery, and biocatalysts and colloid emulsifiers recycling could be easily realized. As an outstanding feature of this platform, the utilization of NIR/visible light to perform the emulsion inversion without any chemical auxiliaries or temperature variation showed little damage toward the biocatalysts, which was highlighted by the high catalytic efficiency and high enantioselectivity even after 10 cycles.

dx.doi.org/10.1021/ja503123m | J. Am. Chem. Soc. 2014, 136, 7498−7504

This remote controlled inversion method provides a unique toolbox for biphasic enantioselective biocatalysis.

RESULTS AND DISCUSSION

Spiropyrans are one of the most commonly employed photochromic families in photochemistry.[45,46] In this study, a carboxyl containing spiropyran (Sp-COOH) was synthesized as shown in Scheme S1 and Figure S1 according to our previous report.[47] Different from conventional studies, where UV light (λ < 450 nm) was used to induce the isomerization of the "closed" spiropyran form, here NIR excited UCNPs were utilized as UV sources. Herein, $NaYF_4$:Yb, Tm was chosen as the upconversion nanophosphor and was prepared via the thermal decomposition method according to the literature.[30] Transmission electron microscopy (TEM) images of the UCNPs demonstrated their size of about 80 nm (Figure 1a).

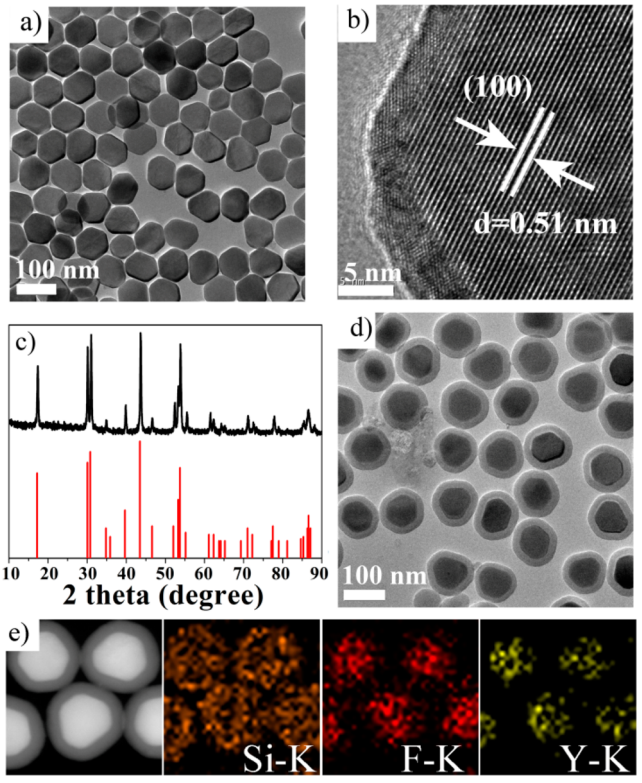

Figure 1. (a) TEM and (b) HRTEM images of oleic acid capped UCNPs; (c) X-ray diffraction pattern of UCNPs ($NaYF_4$:25% Yb, 0.3% Tm) and the standard pattern of β-$NaYF_4$ (JCPDS no. 16-0334); (d) TEM of the synthesized UCNP@SiO_2; (e) dark-field TEM image of UCNP@SiO_2, and corresponding TEM elemental mappings of the Si K-edge, F–K edge and Y K-edge signals.

The X-ray diffraction peaks of UCNPs correlated well with the hexagonal structure of $NaYF_4$ (JCPDS No. 16-0334), which was also confirmed by the high-resolution TEM (HRTEM) image (Figure 1b,c). Then, as shown in Scheme S2, silica was coated onto the nanoparticles by microemulsion method[44] as shown by TEM with an overall size of approximately 110 nm and a shell of about 15 nm (Figure 1d). Meanwhile, energy dispersive spectroscopic (EDS) element mappings of Si, F, and Y further evidenced the UCNP@SiO_2 structure (Figure 1e), in which Si spread everywhere, whereas F and Y only existed in the center of the nanoparticle. Afterward, the surfaces of the resulting nanohybrids were modified by (3-aminopropyl)-triethoxysilane[48] to obtain amino-functionalized UCNP@SiO_2 (UCNP@SiO_2–NH_2) for conjugation of Sp-COOH through EDC/NHS chemistry. The successful grafting of Sp-COOH onto UCNP@SiO_2 was confirmed by FTIR spectroscopy (Figure S2). The typical aryl nitro stretching (1338, 1522 cm^{-1}) and acylamide vibration (1650 cm^{-1}) indicated that spiropyrans have been successfully introduced on the surface of UCNP@SiO_2. By measuring the UV–vis absorption at 337 nm, we determined the grafting amount of Sp-COOH on UCNP@SiO_2 to be 7.6 wt % (Figure S3).

We next assessed the optical properties of spiropyran decorated UCNP@SiO_2 (denoted as Sp-UCNPs). UV–vis absorption spectroscopy of the ring-closed spiropyran showed an absorption peak around 350 nm which overlaps well with the emissions of UCNPs in the UV region attributed to $^3I_6 \rightarrow {}^3F_4$ and $^1D_2 \rightarrow {}^3H_6$ transitions of Tm^{3+} ions (Figure 2a). This

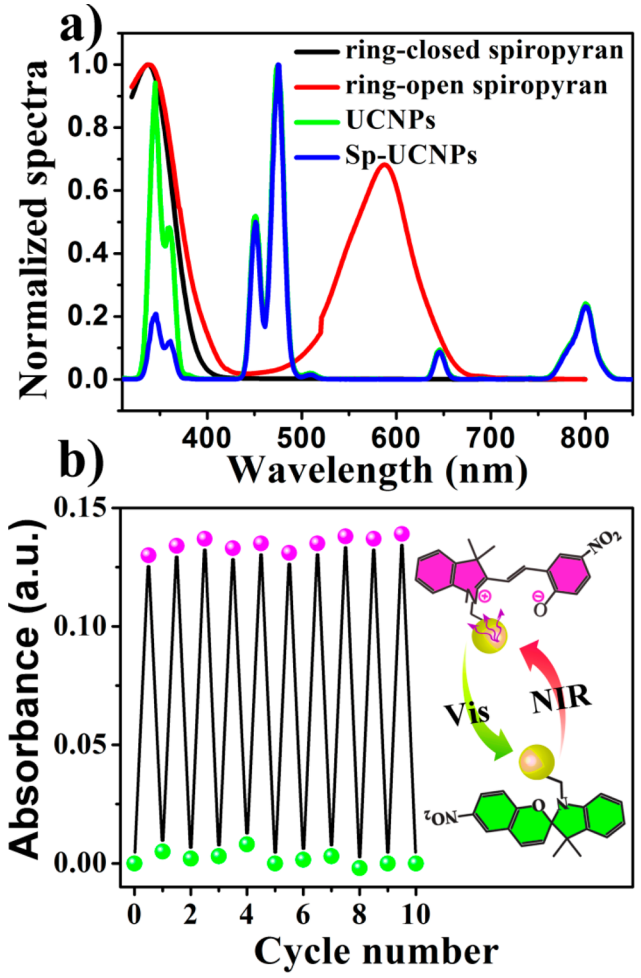

Figure 2. (a) UV–vis absorption spectra of ring-closed and ring-open spiropyran in THF solvent, and the upconversion emission spectrum of UCNPs and Sp-UCNPs. (b) Irradiation cycles of Sp-UCNPs under alternate 980 nm and visible light irradiation.

suggested that the NIR excited UCNPs could be used to trigger the spiropyran → merocyanine switch through energy transfer process. The energy transfer process was confirmed by the observation of emission quenching of the particle solution upon NIR excitation and the energy transfer efficiency was calculated to be 78% (Figure 2a). As shown in Figure S4, a new absorption band around 560 nm appeared upon NIR

dx.doi.org/10.1021/ja503123m | J. Am. Chem. Soc. 2014, 136, 7498–7504

irradiation of the suspension of Sp-USNPs conjugates in toluene; the absorption strength increased with prolonged time and reached equilibrium by 6 min and the solution changed from colorless to violet. The photoswitching behavior of Sp-UCNP was examined by monitoring the optical density at 560 nm which was a quantitative measure of the merocyanine form following alternating NIR/visible irradiation (10 cycles). Figure 2b showed that transformation with NIR and visible light was reversible and did not adversely affect the efficiency of the switching, indicating the excellent photostability of conjugated spiropyrans. This good repeatability was necessary for the remote controlled reversible inversion of Pickering emulsions stabilized by Sp-UCNPs.

We next examined the interfacial activity and the remote controlled reversible inversion ability of the Pickering emulsions stabilized by Sp-UCNP conjugates. Typically, 1.5 mL of water was added into equal volume of toluene containing 1.0 wt % of Sp-UCNPs, followed by homogenizing to give w/o emulsions under indoor ambient conditions (exposed to visible light). As shown in Figure 3a, Sp-UCNPs stabilized emulsions

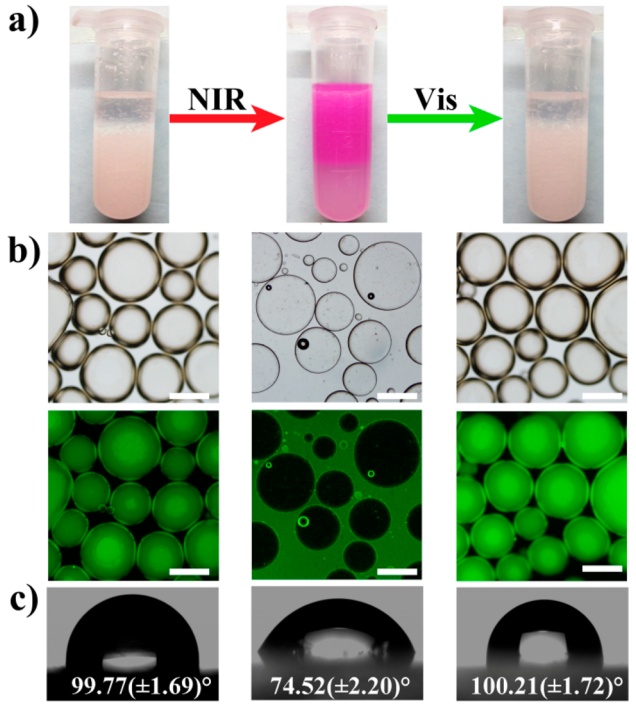

Figure 3. (a) Photograph of Sp-UCNPs stabilized Pickering emulsions: w/o (left), o/w (middle), and w/o (right), where different light was utilized as stimuli before homogenization. (b) Fluorescence microscopy images of the corresponding Pickering emulsions shown in (a) (scale bar: 200 μm). (c) Water contact angles of Sp-UCNPs treated with the corresponding wavelength of light used in (a); the data are averages of at least 10 measurements at different places on the each sample. See experimental section in Supporting Information for details.

were well distributed in the bottom layer with good stability against sedimentation (at least 2 weeks). Interestingly, upon 980 nm irradiation and homogenization, Sp-UCNPs transferred to the upper layer where pink emulsions were observed, indicating the formation of o/w emulsions. More interestingly, Sp-UCNPs could again transfer back to the bottom layer after exposing to visible light and shaking, where colorless w/o emulsions were observed. In control experiments, neither UCNP@SiO_2 nor UCNP@SiO_2–NH_2 stabilized emulsions were observed to exhibit NIR/visible light responsive properties (Figure S5a and S6a).

To illustrate the process, dextran labeled with fluorescein isothiocyanate (Dex-FITC) was used to distinguish the water and toluene phases in the fluorescence microscopy images. As shown in Figure 3b, initially, green emission was observed in the droplet, and the w/o Pickering emulsions could be clearly identified. Upon NIR irradiation, the Sp-UCNPs became water-soluble. Following homogenization, o/w emulsions were formed where the outer phase exhibited green fluorescence. When the nanoparticles were exposed to visible light, emulsions were o/w again. The light-triggered double phase inversion was further supported by water contact angle measurements (Figure 3c). The water contact angle of the freshly prepared Sp-UCNPs was 99.77°, whereas the water contact angle of the NIR treated Sp-UCNPs decreased to 74.52°, confirming the hydrophilic properties. When the ring-opened spiropyran conjugated UCNPs were further treated with visible light, the water contact angle went back to 100.21°. As anticipated, such changes drove the Sp-UCNPs stabilized emulsions inversion between o/w and w/o. In contrast, the wettability of UCNP@SiO_2 and UCNP@SiO_2-NH_2 was almost unaffected by either visible or NIR light (Figures S5b and S6b). Correspondingly, the conductivity variation of the continuous phase of Pickering emulsions also demonstrated the inversion processes (Figure S7). All these results confirmed that the NIR and visible light triggered surface hydrophilic/hydrophobic transitions are critically important to this process.

Besides water/toluene system, Sp-UCNPs could also be used to stabilize Pickering emulsions, which utilize ethyl acetate as the oil phase (Figure S9). In the above systems, both kinds of Pickering emulsions could be easily inverted between w/o and o/w by just exposing to different wavelengths of light. More importantly, the inversion was highly reversible. Even after 10 cycles, Pickering emulsions could still be formed (Figures S8 and S9). The excellent recyclability could be attributed to the surface wettability variations of nanoparticles induced by the reversible photochromism and the excellent photostability of the conjugated spiropyran compounds. The present method indeed provided a simple way to manipulate the behavior of particles adsorbed at fluid interfaces. These unique advantages would allow on-demand phase inversion, which are favorable for effectively recycling catalysts and separating products in biphasic reaction systems.

For benchmarking, a biocatalytic active microbe, *A. faecalis* ATCC 8750 (Figure S10) was introduced into this system. ATCC 8750 has an *R*-enantioselective nitrilase, which can enantioselectively hydrolyze racemic mandelonitrile to produce optically active mandelic acid (Figure 4a and Scheme S3), an important chiral building block for the production of pharmaceuticals.[49−51] Although the microbe shows high entioselectivity, the low substrate concentration tolerance of nitrilase (typically ≤40 mM) hinders their further applications.[50,51] Alternatively, substrate inhibition can be countered by the use of a substrate feeding system.[50] Taking into account the poor water solubility of mandelonitrile, we anticipated that Pickering emulsions in which hydrophobic substrate was retained in the organic phase and microorganisms were retained in the aqueous phase would help to minimize the substrate inhibition. Moreover, in case of toluene, the substrate mandelonitrile partitioned mainly in the organic phase; meanwhile, the product mandelic acid mainly dissolved

dx.doi.org/10.1021/ja503123m | J. Am. Chem. Soc. 2014, 136, 7498−7504

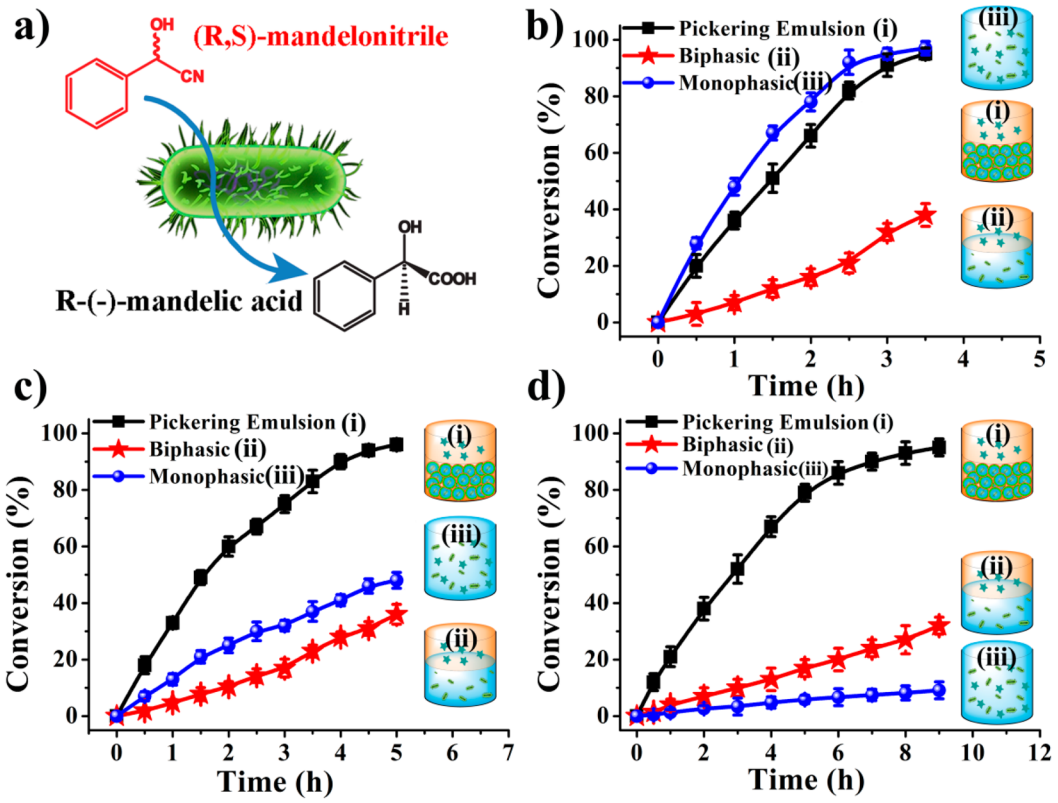

Figure 4. (a) Enantioselective hydrolysis of mandelonitrile to (*R*)-(−)-mandelic acid by *A. faecalis* ATCC 8750. (b–d) Plot of the conversion of the hydrolysis of mandelonitrile catalyzed by ATCC 8750 under different conditions versus reaction time. The initial concentration of mandelonitrile utilized in panels b, c, and d was 50, 100, and 300 mM, respectively. Pickering emulsions and biphasic and monophasic reaction systems were described in detail in the experimental section in Supporting Information.

(>98%) in aqueous phase. Therefore, water/toluene Pickering emulsion system was considered to be more suitable for regulating the substrate concentration around the biocatalyst and facilitating product recovery.

Prior to the enantioselective catalytic studies with ATCC 8750, the viability of the encapsulated microbe was tested with Calcein-AM/Propidium iodide live/dead kit. As shown in Figure S11, significant green fluorescence was visible and no red fluorescence was shown, indicating that most of the encapsulated cells were still viable. The biocatalytic performance of the microbe loaded Pickering emulsions was then investigated with different concentrations of mandelonitrile. Two other experiments where biphasic reaction and monophasic reaction containing free microbes were carried out as negative controls. As shown in Figure 4, the conversion of the reaction in Pickering emulsion systems reached 95% at equilibrium and even the concentration of the substrate was as high as 300 mM. However, after the same time, less than 40% conversion was observed for biphasic reactions without Pickering emulsions. In stark contrast, significant substrate inhibition was observed for monophasic reactions at high substrate concentrations. After normalization (Table S1), the specific activity (μmol·min^{-1}·mg^{-1} dry cell weight, DCW) of the ATCC 8750 loaded in Pickering emulsions was more than 5 times higher than that of native ATCC 8750 in the biphasic water/toluene systems. Moreover, the specific activity of the immobilized ATCC 8750 increased with an increase in the amount of Sp-UCNPs while maintaining the concentration of the biocatalyst (Figure S13 in the Supporting Information). Meanwhile, the average droplet diameter decreased from 870 to 80 μm when the colloidal emulsifier concentration increased from 0.4 to 1.5 wt %. Also, the polydispersity of the emulsion droplets increased simultaneously (Figure S13 in the Supporting Information). In addition, further study of ATCC 8750 kinetics in the Pickering emulsions demonstrated that the reaction obeyed Michaelis–Menten kinetics in a certain range of mandelonitrile concentration (Figure S14 in the Supporting Information). Thus, it can be deduced that substrate inhibition did not appear in the concentration range examined. We therefore rationalized that the significant enhancement of ATCC 8750 biocatalytic activity after immobilization was a result of the drastically increased interfacial area by Pickering emulsions, which improved mass transfer and accessibility of the biocatalyst in the reaction system. Moreover, the organic phase of the Pickering emulsion could serve as an excellent mandelonitrile feeding system for regulating the substrate concentration around biocatalyst, which could effectively protect ATCC 8750 from substrate inhibition at high concentrations.

Another apparent advantage of the Sp-UCNPs stabilized Pickering emulsions for biphasic biocatalytic reactions is the ease of substrate recovery, and biocatalyst and colloid emulsifier recycling. As shown in Scheme S4, at the end of each cycle, NIR irradiation was used to transform the w/o emulsions to o/w emulsions and the extra aqueous was quickly resolved in the bottom layer. Next, the aqueous solvent was removed and the biphasic system was rinsed several times with fresh solvent. The product and biocatalyst in the rinsed aqueous solution were separated through centrifugation. Then, the recovered microbes were dispersed in fresh solvents and introduced again to the

dx.doi.org/10.1021/ja503123m | *J. Am. Chem. Soc.* 2014, 136, 7498–7504

system. Due to its good solubility in toluene, new substrate could be easily added to restart a new cycle. As shown in Figure 5, at the fifth and 10th cycle, the conversions were still 93% and

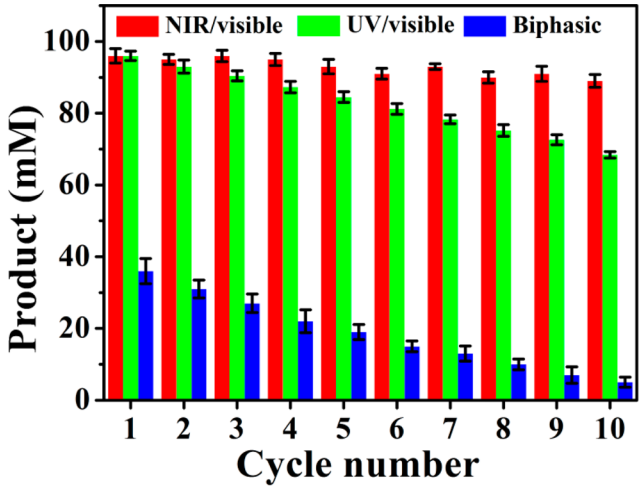

Figure 5. Recycle biocatalytic hydrolysis of mandelonitrile by *A. faecalis* ATCC 8750 in NIR/visible light controlled Pickering emulsions, UV/visible light controlled Pickering emulsions, and water−toluene biphasic systems.

89% in Pickering emulsions, respectively. Quite impressively, during all the cycles, highly optically pure (*R*)-(−)-mandelic acid (ee values are shown in Table S2) was obtained. However, in one control experiment where UV and visible light were used to induce emulsion inversion, the conversion efficiency decreased with increasing cycles. In another control experiment, a similar profile but much lower conversion was observed in the biphasic reaction systems without Pickering emulsion droplets. To better understand the high effectiveness of this method, we determined the viability of the microbes after 5 and 10 reaction cycles by colony-counting method. As can be seen in Figure S16, decreased viability of microbes was observed in both control experiments, whereas the microbes exhibited higher viability from the NIR/visible light controlled Pickering emulsion system. Thus, the loss of biocatalytic activity in control experiments might be attributed to bacteria damage induced by UV light or organic solvents. Therefore, the utilization of NIR/visible light controlled reversible inversion of nanophosphor-stabilized Pickering emulsions greatly enhanced the stability of the biocatalyst and enabled simple product separation and recycling of biocatalyst and emulsifiers.

CONCLUSION

In summary, by tuning the surface chemistry using photochromic spiropyrans, we have successfully prepared interfacially active upconversion nanophosphors for the formulation of Pickering emulsions with NIR/visible light controlled inversion properties. With this multifunctional Pickering emulsion, a model biocatalytic active bacteria *A. faecalis* ATCC 8750 was loaded in the aqueous phase, which not only highly enhanced its catalytic performance but also improved the substrate tolerance. Moreover, product recovery and biocatalysts and emulsifier recycling could be easily realized based on the inversion ability of the Pickering emulsion. Most importantly, the utilization of NIR/visible light to perform the emulsion inversion without any chemical auxiliaries or temperature variation showed little damage toward the biocatalysts, which was highlighted by the high catalytic efficiency and high enantioselectivity even after 10 cycles. We anticipate that this NIR/visible light controlled Pickering emulsion would provide unique opportunities for enantioselective biocatalysis in two-phase systems.

ASSOCIATED CONTENT

Supporting Information

Detailed experimental procedures and supplementary figures and tables. This material is available free of charge via the Internet at http://pubs.acs.org.

AUTHOR INFORMATION

Corresponding Authors

jren@ciac.ac.cn
xqu@ciac.ac.cn

Notes

The authors declare no competing financial interest.

ACKNOWLEDGMENTS

Financial support was provided National Basic Research Program of China (Grant 2012CB72 0602, 2011CB936004) and the National Natural Science Foundation of China (Grants 91213302, 21210002)

REFERENCES

(1) Klibanov, A. M. *Science* **1983**, *219*, 722.
(2) Klibanov, A. M. *Nature* **2001**, *409*, 241.
(3) Schmid, A.; Dordick, J. S.; Hauer, B.; Kiener, A.; Wubbolts, M.; Witholt, B. *Nature* **2001**, *409*, 258.
(4) Liu, J.; Bai, S.; Jin, Q.; Li, C.; Yang, Q. *Chem. Sci.* **2012**, *3*, 3398.
(5) García-Urdiales, E.; Alfonso, I.; Gotor, V. *Chem. Rev.* **2004**, *105*, 313.
(6) Santaniello, E.; Ferraboschi, P.; Grisenti, P.; Manzocchi, A. *Chem. Rev.* **1992**, *92*, 1071.
(7) Sheldon, R. A. *Adv. Synth. Catal.* **2007**, *349*, 1289.
(8) Ansorge-Schumacher, M. B. *Mini-Rev. Org. Chem.* **2007**, *4*, 243.
(9) Khmelnitsky, Y. L.; Hilhorst, R.; Visser, A. J. W. G.; Veeger, C. *Eur. J. Biochem.* **1993**, *211*, 73.
(10) Dinsmore, A. D.; Hsu, M. F.; Nikolaides, M. G.; Marquez, M.; Bausch, A. R.; Weitz, D. A. *Science* **2002**, *298*, 1006.
(11) Wu, C.; Bai, S.; Ansorge-Schumacher, M. B.; Wang, D. *Adv. Mater.* **2011**, *23*, 5694.
(12) Melle, S.; Lask, M.; Fuller, G. G. *Langmuir* **2005**, *21*, 2158.
(13) Duan, H.; Wang, D.; Sobal, N. S.; Giersig, M.; Kurth, D. G.; Möhwald, H. *Nano Lett.* **2005**, *5*, 949.
(14) Lam, S.; Blanco, E.; Smoukov, S. K.; Velikov, K. P.; Velev, O. D. *J. Am. Chem. Soc.* **2011**, *133*, 13856.
(15) Brugger, B.; Richtering, W. *Adv. Mater.* **2007**, *19*, 2973.
(16) Binks, B. P.; Murakami, R.; Armes, S. P.; Fujii, S. *Angew. Chem., Int. Ed.* **2005**, *44*, 4795.
(17) Liu, J.; Lan, G.; Peng, J.; Li, Y.; Li, C.; Yang, Q. *Chem. Commun.* **2013**, *49*, 9558.
(18) Wang, Z.; van Oers, M. C. M.; Rutjes, F. P. J. T.; van Hest, J. C. M. *Angew. Chem., Int. Ed.* **2012**, *51*, 10746.
(19) Scott, G.; Roy, S.; Abul-Haija, Y. M.; Fleming, S.; Bai, S.; Ulijn, R. V. *Langmuir* **2013**, *29*, 14321.
(20) Zhang, C.; Hu, C.; Zhao, Y.; Möller, M.; Yan, K.; Zhu, X. *Langmuir* **2013**, *29*, 15457.
(21) Wiese, S.; Spiess, A. C.; Richtering, W. *Angew. Chem., Int. Ed.* **2013**, *52*, 576.
(22) Kosif, I.; Cui, M.; Russell, T. P.; Emrick, T. *Angew. Chem., Int. Ed.* **2013**, *52*, 6620.
(23) Yang, H.; Zhou, T.; Zhang, W. *Angew. Chem., Int. Ed.* **2013**, *52*, 7455.

(24) Binks, B. P.; Rodrigues, J. A. *Angew. Chem., Int. Ed.* **2005**, *44*, 441.
(25) Jiang, J.; Zhu, Y.; Cui, Z.; Binks, B. P. *Angew. Chem., Int. Ed.* **2013**, *52*, 12373.
(26) Crossley, S.; Faria, J.; Shen, M.; Resasco, D. E. *Science* **2010**, *327*, 68.
(27) Zapata, P. A.; Faria, J.; Ruiz, M. P.; Jentoft, R. E.; Resasco, D. E. *J. Am. Chem. Soc.* **2012**, *134*, 8570.
(28) Zhang, W.; Fu, L.; Yang, H. *ChemSusChem* **2014**, *7*, 391.
(29) Liu, Y.; Chen, M.; Cao, T.; Sun, Y.; Li, C.; Liu, Q.; Yang, T.; Yao, L.; Feng, W.; Li, F. *J. Am. Chem. Soc.* **2013**, *135*, 9869.
(30) Deng, R.; Xie, X.; Vendrell, M.; Chang, Y. T.; Liu, X. *J. Am. Chem. Soc.* **2011**, *133*, 20168.
(31) Liu, J.; Liu, Y.; Liu, Q.; Li, C.; Sun, L.; Li, F. *J. Am. Chem. Soc.* **2011**, *133*, 15276.
(32) Xie, X.; Gao, N.; Deng, R.; Sun, Q.; Xu, Q.; Liu, X. *J. Am. Chem. Soc.* **2013**, *135*, 12608.
(33) Yang, Y.; Velmurugan, B.; Liu, X.; Xing, B. *Small* **2013**, *9*, 2937.
(34) Yang, Y.; Shao, Q.; Deng, R.; Wang, C.; Teng, X.; Cheng, K.; Cheng, Z.; Huang, L.; Liu, Z.; Liu, X.; Xing, B. *Angew. Chem., Int. Ed.* **2012**, *51*, 3125.
(35) Downing, E.; Hesselink, L.; Ralston, J.; Macfarlane, R. *Science* **1996**, *273*, 1185.
(36) Boyer, J. C.; Carling, C. J.; Gates, B. D.; Branda, N. R. *J. Am. Chem. Soc.* **2010**, *132*, 15766.
(37) Wang, C.; Tao, H.; Cheng, L.; Liu, Z. *Biomaterials* **2011**, *32*, 6145.
(38) Zhang, C.; Xu, C. H.; Sun, L. D.; Yan, C. H. *Chem. Asian. J.* **2012**, *7*, 2225.
(39) Cheng, L.; Yang, K.; Li, Y.; Chen, J.; Wang, C.; Shao, M.; Lee, S. T.; Liu, Z. *Angew. Chem., Int. Ed.* **2011**, *50*, 7385.
(40) Liu, Z.; Ju, E.; Liu, J.; Du, Y.; Li, Z.; Yuan, Q.; Ren, J.; Qu, X. *Biomaterials* **2013**, *34*, 7444.
(41) Haase, M.; Schäfer, H. *Angew. Chem., Int. Ed.* **2011**, *50*, 5808.
(42) Zhang, B. F.; Frigoli, M.; Angiuli, F.; Vetrone, F.; Capobianco, J. A. *Chem. Commun.* **2012**, *48*, 7244.
(43) Ju, Q.; Tu, D.; Liu, Y.; Li, R.; Zhu, H.; Chen, J.; Chen, Z.; Huang, M.; Chen, X. *J. Am. Chem. Soc.* **2011**, *134*, 1323.
(44) Mahalingam, V.; Vetrone, F.; Naccache, R.; Speghini, A.; Capobianco, J. A. *Adv. Mater.* **2009**, *21*, 4025.
(45) Xia, F.; Guo, W.; Mao, Y.; Hou, X.; Xue, J.; Xia, H.; Wang, L.; Song, Y.; Ji, H.; Ouyang, Q.; Wang, Y.; Jiang, L. *J. Am. Chem. Soc.* **2008**, *130*, 8345.
(46) Yuan, W.; Sun, L.; Tang, H.; Wen, Y.; Jiang, G.; Huang, W.; Jiang, L.; Song, Y.; Tian, H.; Zhu, D. *Adv. Mater.* **2005**, *17*, 156.
(47) Song, Y.; Xu, C.; Wei, W.; Ren, J.; Qu, X. *Chem. Commun.* **2011**, *47*, 9083.
(48) Lin, Y.; Zhao, A.; Tao, Y.; Ren, J.; Qu, X. *J. Am. Chem. Soc.* **2013**, *135*, 4207.
(49) Yamamoto, K.; Oishi, K.; Fujimatsu, I.; Komatsu, K. *Appl. Environ. Microb.* **1991**, *57*, 3028.
(50) Yamamoto, K.; Fujimatsu, I.; Komatsu, K. I. *J. Ferment. Bioeng.* **1992**, *73*, 425.
(51) Zhang, Z. J.; Xu, J. H.; He, Y. C.; Ouyang, L. M.; Liu, Y. Y.; Imanaka, T. *Process Biochem.* **2010**, *45*, 887.